

Reducing the spectral index in F-term hybrid inflation through a complementary modular inflation

G. Lazarides^{1,*} and C. Pallis^{2,†}

¹*Physics Division, School of Technology, Aristotle University of Thessaloniki, Thessaloniki 54124, Greece*

²*School of Physics and Astronomy, The University of Manchester, Manchester M13 9PL, United Kingdom*

We consider two-stage inflationary models in which a superheavy scale F-term hybrid inflation is followed by an intermediate scale modular inflation. We confront these models with the restrictions on the power spectrum $P_{\mathcal{R}}$ of curvature perturbations and the spectral index n_s implied by the recent data within the power-law cosmological model with cold dark matter and a cosmological constant. We show that these restrictions can be met provided that the number of e-foldings N_{HI^*} suffered by the pivot scale $k_* = 0.002/\text{Mpc}$ during hybrid inflation is appropriately restricted. The additional e-foldings required for solving the horizon and flatness problems can be naturally generated by the subsequent modular inflation. For central values of $P_{\mathcal{R}}$ and n_s , we find that, in the case of standard hybrid inflation, the values obtained for the grand unification scale are close to its supersymmetric value $M_{\text{GUT}} = 2.86 \times 10^{16}$ GeV, the relevant coupling constant is relatively large ($\approx 0.005 - 0.14$), and $10 \lesssim N_{\text{HI}^*} \lesssim 21.7$. In the case of shifted [smooth] hybrid inflation, the grand unification scale can be identified with M_{GUT} provided that $N_{\text{HI}^*} \simeq 21$ [$N_{\text{HI}^*} \simeq 18$].

PACS numbers: 98.80.Cq

1. INTRODUCTION

The recently announced three-year results [1] from the Wilkinson microwave anisotropy probe (WMAP3) bring under considerable stress the well-motivated, popular, and quite natural models [2] of supersymmetric (SUSY) F-term hybrid inflation (FHI) [3], realized [4] at (or close to) the SUSY grand unified theory (GUT) scale $M_{\text{GUT}} = 2.86 \times 10^{16}$ GeV. This is due to the fact that, in these models, the predicted spectral index n_s is too close to unity and without much running. Moreover, in the presence of non-renormalizable terms generated by supergravity (SUGRA) corrections with canonical Kähler potential, n_s approaches [5] unity more drastically and can even exceed it. This is in conflict with the WMAP3 prediction. Indeed, fitting the WMAP3 data with the standard power-law cosmological model with cold dark matter and a cosmological constant (Λ CDM), one obtains [1] that, at the pivot scale $k_* = 0.002/\text{Mpc}$,

$$n_s = 0.958 \pm 0.016 \Rightarrow 0.926 \lesssim n_s \lesssim 0.99 \quad (1)$$

at 95% confidence level.

A way out of this inconsistency is [6, 7] based on the utilization of a quasi-canonical Kähler potential. With a convenient arrangement of the signs, a negative mass term can be induced [7, 8] in the inflationary potential of the FHI models. As a consequence, the inflationary path acquires a local maximum. Under suitable initial conditions, the so-called hilltop inflation [6] can take place as the inflaton rolls from this maximum down to smaller values. In this case, n_s can become consistent with Eq. (1),

but only at the cost of an extra indispensable mild tuning [8] of the initial conditions. Alternatively, it is suggested [9] that n_s 's between 0.98 and 1 can be made compatible with the data by taking into account a sub-dominant contribution to the curvature perturbation due to cosmic strings, which may be (but are not necessarily [10]) formed during the phase transition at the end of FHI. In such a case, the resulting GUT scale is constrained to values well below the SUSY GUT scale [8, 11, 12].

In this paper, we propose a two-step inflationary setup which allows acceptable n_s 's in the context of the FHI models even with canonical Kähler potential and without cosmic strings. The key point in our proposal is that the total number of e-foldings N_{tot} required for the resolution of the horizon and flatness problems of the standard big bang cosmology does not have to be produced exclusively during the GUT scale FHI. Since n_s within the FHI models generally decreases with the number of e-foldings N_{HI^*} that the pivot scale k_* suffers during FHI, we could constrain N_{HI^*} so that Eq. (1) is satisfied. The residual number of e-foldings $N_{\text{tot}} - N_{\text{HI}^*}$ can be obtained by a second stage of inflation realized at a lower scale. We call this type of inflation, which complements the number of e-foldings produced during the GUT scale inflation, complementary inflation. In our scenario, modular inflation (MI), which can be easily realized [13] by a string axion, plays this role and produces the required additional number of e-foldings $N_{\text{tot}} - N_{\text{HI}^*}$ with natural values of the relevant parameters. Such a construction is also beneficial for MI, since the perturbations of the inflaton in this model are not sufficiently large to account for the observations, due to its low inflationary energy scale. As an extra bonus, the gravitino constraint [14] and the potential topological defect [15] problem of FHI can be significantly relaxed due to the enormous entropy release taking place after MI (which naturally assures a low reheat temperature). However,

*Electronic address: lazaride@eng.auth.gr

†Electronic address: Constantinos.Pallis@manchester.ac.uk

for the same reason, baryogenesis is made more difficult but not impossible [16] in the context of a larger scheme with (large) extra dimensions. It is interesting to note that a constrained N_{HI^*} was previously used in Ref. [17] to achieve a sufficient running of the spectral index. The additional e-foldings were provided by new inflation [18].

Below, we briefly review the basic FHI models (Sec. 2) and describe the calculation of the relevant inflationary observables (Sec. 3). Then, we sketch the main features of MI (Sec. 4) and exhibit the constraints imposed on our cosmological set-up (Sec. 5). We end up with our numerical results (Sec. 6) and conclusions (Sec. 7).

2. THE FHI MODELS

The FHI can be realized [2] adopting one of the superpotentials below:

$$W = \begin{cases} \kappa S (\bar{\Phi}\Phi - M^2) & \text{for standard FHI,} \\ \kappa S (\bar{\Phi}\Phi - M^2) - S \frac{(\bar{\Phi}\Phi)^2}{M_S^2} & \text{for shifted FHI,} \\ S \left(\frac{(\bar{\Phi}\Phi)^2}{M_S^2} - \mu_S^2 \right) & \text{for smooth FHI,} \end{cases} \quad (2)$$

where $\bar{\Phi}, \Phi$ is a pair of left handed superfields belonging to non-trivial conjugate representations of a GUT gauge group G and reducing its rank by their vacuum expectation values (VEVs), S is a gauge singlet left handed superfield, $M_S \sim 5 \times 10^{17}$ GeV is an effective cutoff scale of the order of the string scale, and the parameters κ and $M, \mu_S (\sim M_{\text{GUT}})$ are made positive by field redefinitions.

The superpotential for standard FHI in Eq. (2) is the most general renormalizable superpotential consistent with a global $U(1)$ R symmetry [4] under which

$$S \rightarrow e^{i\alpha} S, \bar{\Phi}\Phi \rightarrow \bar{\Phi}\Phi, W \rightarrow e^{i\alpha} W. \quad (3)$$

Including in the superpotential for standard FHI the leading non-renormalizable term, one obtains the superpotential for shifted [19] FHI in Eq. (2). The superpotential for smooth [20] FHI is produced by further imposing an extra Z_2 symmetry under which $\Phi \rightarrow -\Phi$ and, thus, allowing only even powers of the combination $\bar{\Phi}\Phi$.

From the emerging scalar potential, we can deduce that the vanishing of the D-terms implies that $|\langle \bar{\Phi} \rangle| = |\langle \Phi \rangle|$, while the vanishing of the F-terms gives the VEVs of the fields in the SUSY vacuum (in the case where $\bar{\Phi}, \Phi$ are not standard model (SM) singlets, $\langle \bar{\Phi} \rangle, \langle \Phi \rangle$ stand for the VEVs of their SM singlet directions). These VEVs are $\langle S \rangle = 0$ and $|\langle \bar{\Phi} \rangle| = |\langle \Phi \rangle| = v_G$ with

$$v_G = \begin{cases} M & \text{for standard FHI,} \\ \frac{M}{\sqrt{2\xi}} \sqrt{1 - \sqrt{1 - 4\xi}} & \text{for shifted FHI,} \\ \sqrt{\mu_S M_S} & \text{for smooth FHI,} \end{cases} \quad (4)$$

where $\xi = M^2/\kappa M_S^2$ with $1/7.2 < \xi < 1/4$ [19]. As a consequence, W leads to the spontaneous breaking of G . The same superpotential W gives also rise to hybrid inflation. This is due to the fact that, for large enough values of $|S|$, there exist flat directions i.e. valleys of local minima of the classical potential with constant (or almost constant in the case of smooth FHI) potential energy density. If we call V_{HI0} the dominant contribution to the (inflationary) potential energy density along these directions, we have

$$V_{\text{HI0}} = \begin{cases} \kappa^2 M^4 & \text{for standard FHI,} \\ \kappa^2 M_\xi^4 & \text{for shifted FHI,} \\ \mu_S^4 & \text{for smooth FHI,} \end{cases} \quad (5)$$

with $M_\xi = M\sqrt{1/4\xi - 1}$. Inflation can be realized if a slope along the flat direction (inflationary valley) can be generated for driving the inflaton towards the vacua. In the cases of standard [4] and shifted [19] FHI, this slope can be generated by the SUSY breaking on this valley. Indeed, $V_{\text{HI0}} > 0$ breaks SUSY and gives rise to logarithmic radiative corrections to the potential originating from a mass splitting in the $\bar{\Phi}, \Phi$ supermultiplets. On the other hand, in the case of smooth [20] FHI, the inflationary valley is not classically flat and, thus, there is no need of radiative corrections. Introducing the canonically normalized inflaton field $\sigma = \sqrt{2}|S|$, the relevant correction V_{HIc} to the inflationary potential can be written as follows:

$$V_{\text{HIc}} = \begin{cases} \frac{\kappa^4 M^4 \mathbf{N}}{32\pi^2} \left(2 \ln \frac{\kappa^2 x M^2}{Q^2} + (x+1)^2 \ln(1+x^{-1}) + (x-1)^2 \ln(1-x^{-1}) \right) & \text{for standard FHI,} \\ \frac{\kappa^4 M_\xi^4}{16\pi^2} \left(2 \ln \frac{2\kappa^2 x_\xi M_\xi^2}{Q^2} + (x_\xi+1)^2 \ln(1+x_\xi^{-1}) + (x_\xi-1)^2 \ln(1-x_\xi^{-1}) \right) & \text{for shifted FHI,} \\ -2\mu_S^6 M_S^2 / 27\sigma^4 & \text{for smooth FHI,} \end{cases} \quad (6)$$

where \mathbf{N} is the dimensionality of the representations to which $\bar{\Phi}$ and Φ belong in the case of standard FHI, Q is a renormalization scale, $x = |S|^2/M^2$, and $x_\xi = \sigma^2/M_\xi^2$. Although in our work rather large κ 's are used in the

cases of standard and shifted FHI, renormalization group effects [21] remain negligible.

For minimal Kähler potential, the leading SUGRA correction V_{HIS} to the scalar potential along the inflationary

valley reads [3, 5, 11]

$$V_{\text{HIS}} = V_{\text{HI0}} \frac{\sigma^4}{8m_{\text{P}}^4}, \quad (7)$$

where $m_{\text{P}} \simeq 2.44 \times 10^{18}$ GeV is the reduced Planck scale.

Let us also note that the most important contribution [22] to the inflationary potential from the soft SUSY breaking terms starts [11, 22] playing an important role, in the case of standard FHI, for $\kappa \lesssim 5 \times 10^{-4}$ and so it remains negligibly small in our set-up due to the large κ 's encountered (see Sec. 6). This contribution, in general, does not have [22] a significant effect in the cases of shifted and smooth FHI too.

All in all, the general form of the potential which drives the various versions of FHI reads

$$V_{\text{HI}} = V_{\text{HI0}} + V_{\text{HIc}} + V_{\text{HIS}}. \quad (8)$$

It is worth mentioning that the crucial difference between the standard and the other two realizations of FHI is that, during standard FHI, both $\bar{\Phi}$ and Φ vanish and so the GUT gauge group G is restored. As a consequence, topological defects such as strings [8, 11, 12], monopoles, or domain walls may be produced [20] via the Kibble mechanism [15] during the spontaneous breaking of G at the end of FHI. This is avoided in the other two cases, since the form of W allows the existence of non-trivial inflationary valleys along which G is spontaneously broken (with the appropriate Higgs fields $\bar{\Phi}$ and Φ acquiring non-zero values). Therefore, no topological defects are produced in these cases.

3. THE DYNAMICS OF FHI

Assuming (see below) that all the cosmological scales cross outside the horizon during FHI and are not reprocessed during the subsequent MI, we can apply the standard calculations (see e.g. Ref. [23]) for the inflationary observables of FHI.

Namely, the number of e-foldings $N_{\text{HI}*}$ that the pivot scale k_* suffers during FHI can be found from

$$N_{\text{HI}*} = \frac{1}{m_{\text{P}}^2} \int_{\sigma_f}^{\sigma_*} d\sigma \frac{V_{\text{HI}}}{V'_{\text{HI}}}, \quad (9)$$

where the prime denotes derivation with respect to (w.r.t.) σ , σ_* is the value of σ when the pivot scale k_* crosses outside the horizon of FHI, and σ_f is the value of σ at the end of FHI, which can be found, in the slow-roll approximation, from the condition

$$\max\{\epsilon(\sigma_f), |\eta(\sigma_f)|\} = 1, \quad \text{where} \\ \epsilon \simeq \frac{m_{\text{P}}^2}{2} \left(\frac{V'_{\text{HI}}}{V_{\text{HI}}} \right)^2 \quad \text{and} \quad \eta \simeq m_{\text{P}}^2 \frac{V''_{\text{HI}}}{V_{\text{HI}}}. \quad (10)$$

In the cases of standard [4] and shifted [19] FHI, the end of inflation coincides with the onset of the GUT

phase transition, i.e. the slow-roll conditions are violated infinitesimally close to the critical point $\sigma_c = \sqrt{2}M$ [$\sigma_c = M\xi$] for standard [shifted] FHI, where the waterfall regime commences (this is valid even in the case where the term in Eq. (7) plays an important role). On the contrary, the end of smooth [20] FHI is not abrupt since the inflationary path is stable w.r.t. variations in $\bar{\Phi}$, Φ for all σ 's and σ_f is found from Eq. (10).

The power spectrum $P_{\mathcal{R}}$ of the curvature perturbation can be calculated at the pivot scale k_* by

$$P_{\mathcal{R}}^{1/2} = \frac{1}{2\sqrt{3}\pi m_{\text{P}}^3} \left. \frac{V_{\text{HI}}^{3/2}}{|V'_{\text{HI}}|} \right|_{\sigma=\sigma_*}. \quad (11)$$

Finally, the spectral index n_s and its running $dn_s/d\ln k$ are given by

$$n_s = 1 - 6\epsilon(\sigma_*) + 2\eta(\sigma_*) \quad \text{and} \\ dn_s/d\ln k = 2(4\eta(\sigma_*)^2 - (n_s - 1)^2)/3 - 2\xi(\sigma_*) \quad (12)$$

respectively with $\xi \simeq m_{\text{P}}^4 V'_{\text{HI}} V''_{\text{HI}} / V_{\text{HI}}^2$.

4. THE BASICS OF MI

After the gravity mediated soft SUSY breaking, the potential which can support MI has the form [13]

$$V_{\text{MI}} = V_{\text{MI0}} - \frac{1}{2} m_s^2 s^2 + \dots, \quad (13)$$

where the ellipsis denotes terms which are expected to stabilize V_{MI} at $s \sim m_{\text{P}}$ with s being the canonically normalized real string axion field. Therefore, in the above formula, we have

$$V_{\text{MI0}} = v_s (m_{3/2} m_{\text{P}})^2 \quad \text{and} \quad m_s \sim m_{3/2}, \quad (14)$$

where $m_{3/2} \sim 1$ TeV is the gravitino mass and the coefficient v_s is of order unity, yielding $V_{\text{MI0}}^{1/4} \simeq 3 \times 10^{10}$ GeV. In this model, inflation can be of the fast-roll type [24]. The field evolution is given [24] by

$$s = s_i e^{F_s \Delta N_{\text{MI}}} \quad \text{with} \quad F_s \equiv \sqrt{\frac{9}{4} + \left(\frac{m_s}{H_s} \right)^2} - \frac{3}{2}. \quad (15)$$

Here s_i is the initial value of s (i.e. the value of s at the onset of MI), $H_s \simeq \sqrt{V_{\text{MI0}}}/\sqrt{3}m_{\text{P}}$ is the Hubble parameter corresponding to V_{MI0} , and ΔN_{MI} is the number of e-foldings obtained from $s = s_i$ until a given s .

From Eq. (15), we can estimate the total number of e-foldings during MI as

$$N_{\text{MI}} \simeq \frac{1}{F_s} \ln \left(\frac{s_f}{s_i} \right), \quad (16)$$

where s_f is the final value of s . This value is given by $s_f = \min\{\langle s \rangle, s_{\text{sr}}\}$, where $\langle s \rangle \sim m_{\text{P}}$ is the VEV of s and s_{sr} is determined by the condition

$$\epsilon_{\text{MI}} = 1 \quad \text{with} \quad \epsilon_{\text{MI}} \equiv -\frac{\dot{H}_{\text{MI}}}{H_{\text{MI}}^2} \simeq \frac{1}{2} F_s^2 \left(\frac{s}{m_{\text{P}}} \right)^2 \quad (17)$$

being the slow-roll parameter for MI (H_{MI} is the Hubble parameter during MI and the dot denotes derivation w.r.t. the cosmic time). To derive Eq. (17), we use the equation of motion for s during MI and Eq. (15). For definiteness, we take $\langle s \rangle = m_{\text{P}}$ in our calculation.

5. OBSERVATIONAL CONSTRAINTS

The cosmological scenario under consideration needs to satisfy a number of constraints. These can be outlined as follows:

- (a) The power spectrum in Eq. (11) is to be confronted with the WMAP3 data [1]

$$P_{\mathcal{R}}^{1/2} \simeq 4.86 \times 10^{-5} \quad \text{at } k_* = 0.002/\text{Mpc}. \quad (18)$$

- (b) According to the inflationary paradigm, the horizon and flatness problems of the standard big bang cosmology can be successfully resolved provided that the pivot scale k_* suffers a certain total number of e-foldings N_{tot} , which depends on some details of the cosmological scenario. In our set-up, N_{tot} consists of two contributions:

$$N_{\text{tot}} = N_{\text{HI}^*} + N_{\text{MI}}. \quad (19)$$

Employing standard methods [3, 25], we can easily derive, in our case, the required N_{tot} :

$$N_{\text{tot}} \simeq 22.6 + \frac{2}{3} \ln \frac{V_{\text{HI0}}^{1/4}}{1 \text{ GeV}} + \frac{1}{3} \ln \frac{T_{\text{Mrh}}}{1 \text{ GeV}}, \quad (20)$$

where T_{Mrh} is the reheat temperature after the completion of MI. Here, we have assumed that the reheat temperature after FHI is lower than $V_{\text{MI0}}^{1/4}$ (as in the majority of these models [5]) and, therefore, the whole inter-inflationary period is matter dominated.

- (c) We have also to assure that all the cosmological scales (i) leave the horizon during FHI and (ii) do not re-enter the horizon before the onset of MI (this would be possible since the scale factor increases faster than the horizon during the inter-inflationary era [25]). Both these requirements can be met if we demand [25, 26] that

$$N_{\text{HI}^*} \gtrsim N_{\text{HI}^*}^{\text{min}} \simeq 3.9 + \frac{1}{6} \ln \frac{V_{\text{HI0}}}{V_{\text{MI0}}}. \quad (21)$$

The first term in the expression for $N_{\text{HI}^*}^{\text{min}}$ is the number of e-foldings elapsed between the horizon crossing of the pivot scale k_* and the scale $0.1/\text{Mpc}$ during FHI. Note that length scales of the order of 10 Mpc are starting to feel nonlinear effects and it is, thus, difficult to constrain [26] primordial density fluctuations on smaller scales. Given that $(V_{\text{HI0}}/V_{\text{MI0}})^{1/4} \sim 10^{14}/10^{10} \sim 10^4$, we expect that $N_{\text{HI}^*}^{\text{min}} \sim 10$.

- (d) As it is well known [21], in the models under consideration, $|dn_s/d \ln k|$ increases as N_{HI^*} decreases. Therefore, limiting ourselves to $|dn_s/d \ln k|$'s consistent with the assumptions of the power-law ΛCDM cosmological model, we obtain a lower bound on N_{HI^*} . Since, within the cosmological models with running spectral index, $|dn_s/d \ln k|$'s of order 0.01 are encountered [1], we impose the following upper bound on $|dn_s/d \ln k|$:

$$|dn_s/d \ln k| \ll 0.01. \quad (22)$$

In our numerical investigation (see Sec. 6), we display boundary curves for $dn_s/d \ln k = -0.005$ and -0.01 .

- (e) For MI to be natural, we constrain the dimensionless parameter v_s in Eq. (14) as follows:

$$0.5 \leq v_s \leq 10 \quad \Rightarrow \quad 2.45 \gtrsim m_s/H_s \gtrsim 0.55, \quad (23)$$

where we take $m_s = m_{3/2}$ (see below). The lower bound on v_s is chosen so that the sum of the two explicitly displayed terms in the right hand side of Eq. (13) is positive for $s < m_{\text{P}}$. From Eq. (17), we see that, for the values of m_s/H_s in Eq. (23), $s_{\text{sr}} > m_{\text{P}}$ and, thus, $s_{\text{f}} = m_{\text{P}}$. Using Eq. (16), we then find that the upper bound on m_s/H_s implies the constraint $N_{\text{MI}} \gtrsim 0.73 \ln(m_{\text{P}}/s_i)$. Note, though, that Eqs. (15)–(17) are not very accurate near the upper bound on m_s/H_s since, in this region, the slow-roll parameter ϵ_{MI} gets too close to unity at $s = m_{\text{P}}$ and, thus, the Hubble parameter does not remain constant as s approaches m_{P} . So our results at large values of m_s/H_s should be considered only as indicative. Fortunately, as we will see below, the interesting solutions are found near the lower bound on m_s/H_s , where the accuracy of these formulas is much better (of the order of a few per cent for $s_i \sim 0.01 m_{\text{P}}$). Moreover, the slow-roll parameter for MI

$$\eta_{\text{MI}} \equiv m_{\text{P}}^2 \frac{V_{\text{MI}}^{(2)}}{V_{\text{MI}}} \simeq -\frac{1}{3} \left(\frac{m_s}{H_s} \right)^2, \quad (24)$$

where we again take $m_s = m_{3/2}$, satisfies the inequality $|\eta_{\text{MI}}| \leq 1$ for $m_s/H_s \lesssim 1.73$ (the superscript (n) denotes the n th derivative w.r.t. the string axion s). So the interesting solutions correspond to slow- rather than fast-roll MI. We should also point out that the presence of the (unspecified) terms in the ellipsis in the right hand side of Eq. (13), which are needed for stabilizing the potential at $s \sim m_{\text{P}}$, also generates an uncertainty in Eqs. (15)–(17). We assume that this uncertainty is small and neglect it.

- (f) Finally, we assume that FHI lasts long enough so that the value of the almost massless string axion s is completely randomized [27] as a consequence

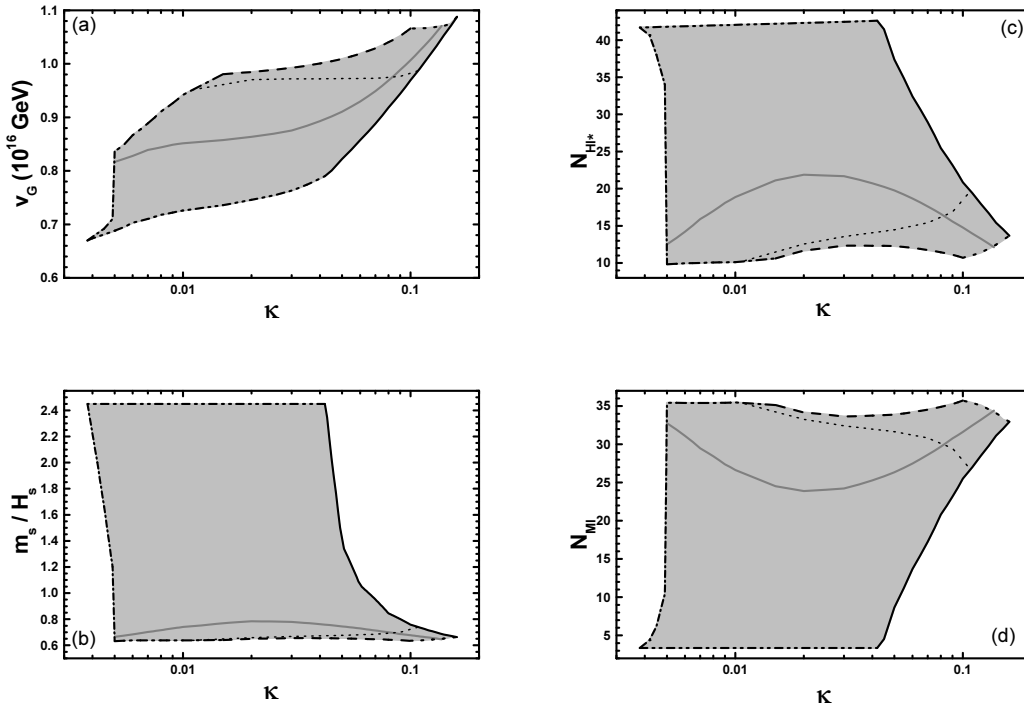


FIG. 1: Allowed (lightly gray shaded) regions in the (a) $\kappa - v_G$, (b) $\kappa - m_s/H_s$, (c) $\kappa - N_{\text{HI}^*}$, and (d) $\kappa - N_{\text{MI}}$ plane for standard FHI. The black solid [dashed] lines correspond to the upper [lower] bound on n_s in Eq. (1), whereas the gray solid lines have been obtained by fixing n_s to its central value in Eq. (1). The dot-dashed [double dot-dashed] lines correspond to the lower [upper] bound on N_{HI^*} [m_s/H_s] from Eq. (21) [Eq. (23)]. The bold [faint] dotted lines correspond to $dn_s/d\ln k = -0.01$ [$dn_s/d\ln k = -0.005$]. Finally, the short dash-dotted lines correspond to the lower bound on V_{HI0} from Eq. (25). In the allowed regions, Eqs. (18) and (20) are also satisfied.

of its quantum fluctuations from FHI. We further assume that

$$V_{\text{MI0}} \lesssim H_{\text{HI0}}^4, \quad (25)$$

where $H_{\text{HI0}} = \sqrt{V_{\text{HI0}}}/\sqrt{3}m_{\text{P}}$ is the Hubble parameter corresponding to V_{HI0} , so that all the values of s belong to the randomization region [27]. The field s remains practically frozen during the inter-inflationary period since the Hubble parameter is larger than its mass. Under these circumstances, all the initial values s_i of s from zero to m_{P} are equally probable. However, we take $s_i \gg H_{\text{HI0}}/2\pi$ so that the homogeneity of our present universe is not jeopardized by the quantum fluctuations of s from FHI. Note that randomization of the value of a scalar field via inflationary quantum fluctuations requires that this field remains almost massless during inflation. For this, it is important that the field does not acquire [3, 28] mass of the order of the Hubble parameter via the SUGRA scalar potential. This is, indeed, the case for the string axion during FHI (and the subsequent inter-inflationary era). In the opposite case, this field could decrease to very small values until the onset of MI as the inflaton of new inflation [18] in Refs. [17, 29].

6. NUMERICAL RESULTS

In the case of standard FHI, we take $\mathbf{N} = 2$. This corresponds to the left-right symmetric GUT gauge group $\text{SU}(3)_c \times \text{SU}(2)_L \times \text{SU}(2)_R \times \text{U}(1)_{\text{B-L}}$ with $\bar{\Phi}$ and Φ belonging to $\text{SU}(2)_R$ doublets with $B - L = -1$ and 1 respectively. It is known [10] that no cosmic strings are produced during this realization of standard FHI. As a consequence, we are not obliged to impose extra restrictions on the parameters (as e.g. in Refs. [11, 12]). Let us mention, in passing, that, in the case of shifted [19] FHI, the GUT gauge group is the Pati-Salam group $\text{SU}(4)_c \times \text{SU}(2)_L \times \text{SU}(2)_R$. We take $T_{\text{Mrh}} = 1$ GeV and $m_{3/2} = m_s = 1$ TeV throughout. These are indicative values which do not affect crucially our results. Indeed, T_{Mrh} appears in Eq. (20) through its logarithm and so its variation has a minor influence on the value of N_{tot} . Furthermore, N_{MI} depends crucially only on F_s – see Eq. (16) – which in turn depends on the ratio m_s/H_s and not separately on m_s or H_s . Finally, we choose the initial value s_i of the string axion s at the onset of MI to be given by $s_i = 0.01 m_{\text{P}}$ in all the cases that we consider. This value is close enough to m_{P} to have a non-negligible probability to be achieved by the randomization of s during FHI (see point (f) in Sec. 5). At the same time, it

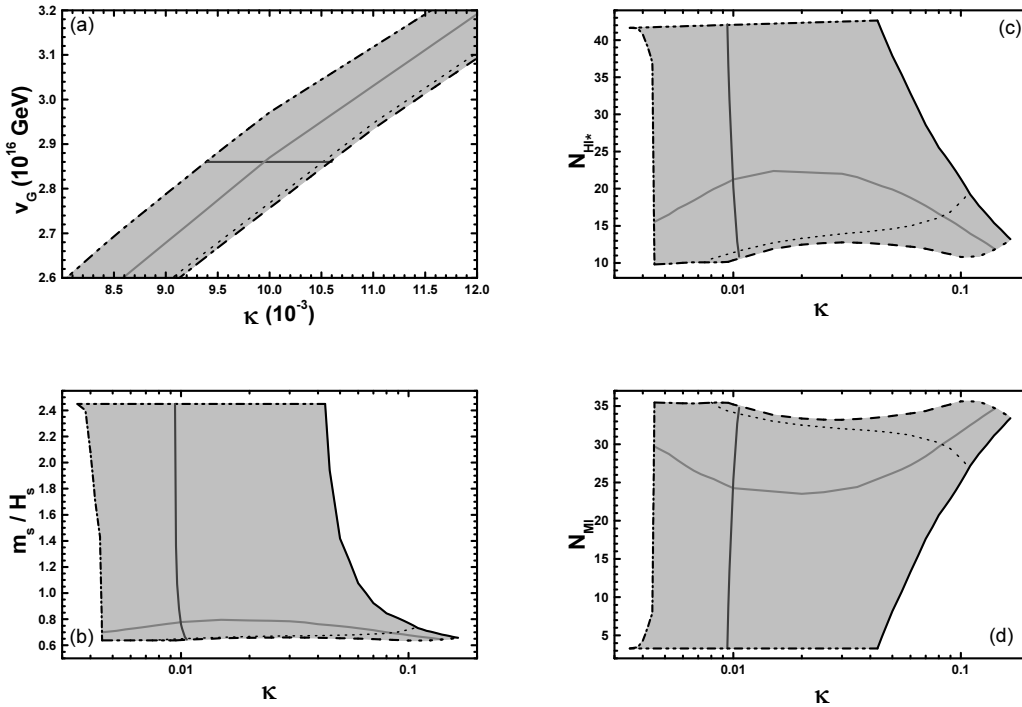


FIG. 2: Allowed regions in the (a) $\kappa - v_G$, (b) $\kappa - m_s/H_s$, (c) $\kappa - N_{\text{HI}^*}$, and (d) $\kappa - N_{\text{MI}}$ plane for shifted FHI with $M_S = 5 \times 10^{17}$ GeV. The notation is the same as in Fig. 1. We also include dark gray solid lines corresponding to $v_G = M_{\text{GUT}}$.

TABLE I: Convention for the various lines in Figs. 1–3.

Type of Line	Corresponding Condition
Black Solid	Upper bound on n_s in Eq. (1)
Dashed	Lower bound on n_s in Eq. (1)
Short Dash-dotted	Lower bound on $V_{\text{HI}0}$ from Eq. (25)
Bold Dotted	$dn_s/d \ln k = -0.01$
Faint Dotted	$dn_s/d \ln k = -0.005$
Dot-dashed	Lower bound on N_{HI^*} in Eq. (21)
Double Dot-dashed	Upper bound on m_s/H_s in Eq. (23)
Gray Solid	Central value of n_s in Eq. (1)
Dark Gray Solid	$v_G = M_{\text{GUT}} = 2.86 \times 10^{16}$ GeV

is adequately smaller than m_P to guarantee good accuracy of Eqs. (15)–(17) near the interesting solutions and justify the fact that we neglect the uncertainty from the terms in the ellipsis in Eq. (13) (see point (e) in Sec. 5). Moreover, larger s_i 's lead to smaller parameter space for interesting solutions (with n_s near its central value).

In our numerical computation, we use, as input parameters, κ (for standard and shifted FHI with fixed $M_S = 5 \times 10^{17}$ GeV) or M_S (for smooth FHI) and σ_* . Using Eqs. (12) and (18), we extract n_s and v_G respectively. For every chosen κ or M_S , we then restrict σ_* so as to achieve n_s in the range of Eq. (1) and take the output values of N_{HI^*} (contrary to the conventional strategy –

see e.g. Refs. [11, 22] – in which $N_{\text{HI}^*} \simeq 53$ is treated as a constraint and n_s is an output parameter). Finally, we find, from Eqs. (19) and (20), the required N_{MI} and the corresponding v_s or m_s/H_s from Eq. (16).

Our results for the three versions of FHI are presented in Figs. 1–3. The conventions adopted for the various lines are displayed in Table I. In Fig. 2(a) [Fig. 3(a)], we focus on a limited range of κ 's [M_S 's] for the sake of clarity of the presentation. Let us discuss each case separately:

Standard FHI. In Fig. 1, we present the regions allowed by Eqs. (1), (18)–(23), and (25) in the (a) $\kappa - v_G$, (b) $\kappa - m_s/H_s$, (c) $\kappa - N_{\text{HI}^*}$, and (d) $\kappa - N_{\text{MI}}$ plane for standard FHI. We observe that (i) the resulting v_G 's and κ 's are restricted to rather large values compared to those allowed within the conventional (i.e. when $N_{\text{MI}} = 0$) set-up (compare with Refs. [11, 22]), (ii) as κ increases above 0.01 the SUGRA corrections in Eq. (7) become more and more significant, (iii) as κ decreases below about 0.015 [0.042] the constraint from the lower [upper] bound on n_s in Eq. (1) ceases to restrict the parameters, since it is overshadowed by the lower [upper] bound on N_{HI^*} [m_s/H_s] in Eq. (21) [Eq. (23)] (indeed, on the dot-dashed lines $9.84 \lesssim N_{\text{HI}^*} = N_{\text{HI}}^{\text{min}} \lesssim 10.62$, which implies that $0.949 \gtrsim n_s \gtrsim 0.926$, while on the double dot-dashed ones $m_s/H_s \simeq 2.45 \Rightarrow N_{\text{MI}} \simeq 3.35$ yielding $n_s \simeq 0.98 - 0.99$), (iv) $|dn_s/d \ln k|$ remains well below the bound in Eq. (22) in the largest part of the regions allowed by the other constraints, whereas $-0.005 \gtrsim dn_s/d \ln k \gtrsim -0.01$ in a very

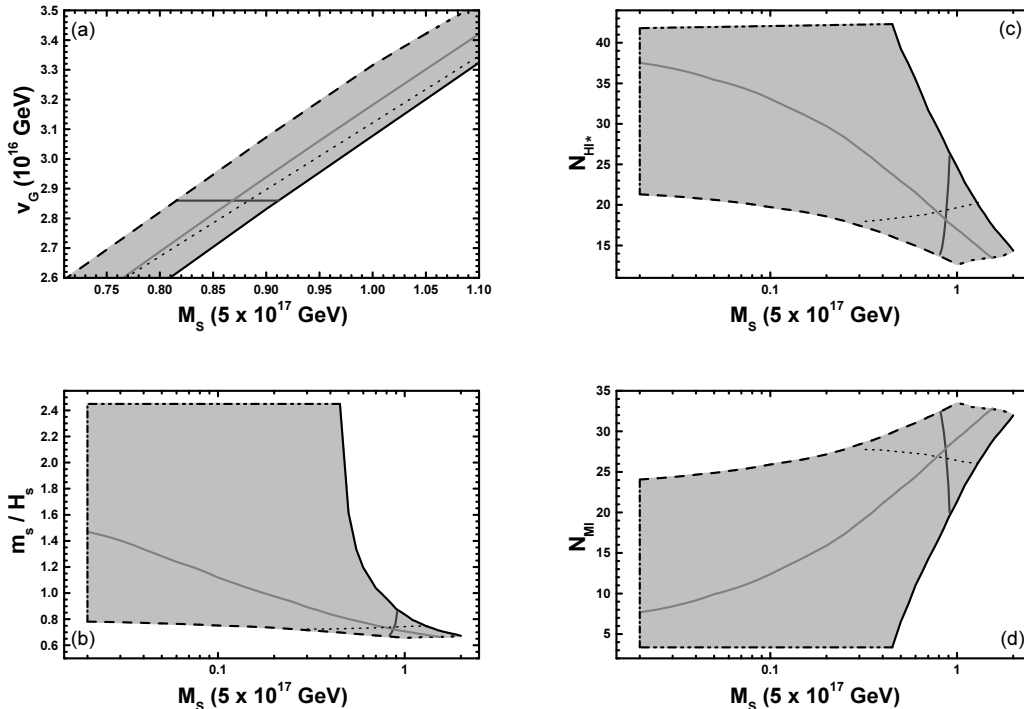


FIG. 3: Allowed regions in the (a) $M_S - v_G$, (b) $M_S - m_s/H_s$, (c) $M_S - N_{\text{HI}^*}$, and (d) $M_S - N_{\text{MI}}$ plane for smooth FHI. The notation is the same as in Fig. 2. We included small M_S 's of less physical interest just to show the effect of the constraints.

TABLE II: Input and output parameters for our scenario with shifted ($M_S = 5 \times 10^{17}$ GeV) or smooth FHI for $n_s = 0.958$ and $v_G = M_{\text{GUT}}$.

Shifted FHI		Smooth FHI	
σ_* (10^{16} GeV)	2.2	σ_* (10^{16} GeV)	23.53
κ	0.01	M_S (5×10^{17} GeV)	0.87
M (10^{16} GeV)	2.35	μ_S (10^{16} GeV)	0.188
$1/\xi$	4.54	σ_f (10^{16} GeV)	13.42
N_{HI^*}	21	N_{HI^*}	18
$dn_s/d \ln k$	-0.0018	$dn_s/d \ln k$	-0.0055
N_{MI}	24.3	N_{MI}	27.8
m_s/H_s	0.77	m_s/H_s	0.72

limited part of these regions, and (v) for $n_s = 0.958$, we obtain $0.004 \lesssim \kappa \lesssim 0.14$, $0.79 \lesssim v_G/(10^{16} \text{ GeV}) \lesssim 1.08$, and $-0.002 \gtrsim dn_s/d \ln k \gtrsim -0.01$ as well as $10 \lesssim N_{\text{HI}^*} \lesssim 21.7$, $35 \gtrsim N_{\text{MI}} \gtrsim 24$, and $0.64 \lesssim m_s/H_s \lesssim 0.77$.

Shifted FHI. In Fig. 2, we delineate the regions allowed by Eqs. (1), (18)–(23), and (25) in the (a) $\kappa - v_G$, (b) $\kappa - m_s/H_s$, (c) $\kappa - N_{\text{HI}^*}$, and (d) $\kappa - N_{\text{MI}}$ plane for shifted FHI with $M_S = 5 \times 10^{17}$ GeV. We observe that (i) in contrast to the case of standard FHI, the lower [upper] bound on N_{HI^*} [m_s/H_s] in Eq. (21) [Eq. (23)] gives a lower [upper] bound on v_G in the $\kappa - v_G$ plane, (ii) the results on m_s/H_s , N_{HI^*} , and N_{MI} are quite similar to those for standard FHI (note that the bounds on ξ do not

cut out any slices of the allowed parameter space), and (iii) v_G comes out considerably larger than in the case of standard FHI and can be equal to the SUSY GUT scale (some key inputs and outputs for the interesting case $v_G = M_{\text{GUT}}$ with $n_s = 0.958$ are presented in Table II).

Smooth FHI. In Fig. 3, we present the regions allowed by Eqs. (1), (18)–(23), and (25) in the (a) $M_S - v_G$, (b) $M_S - m_s/H_s$, (c) $M_S - N_{\text{HI}^*}$, and (d) $M_S - N_{\text{MI}}$ plane for smooth FHI. We observe that (i) the SUGRA corrections in Eq. (7) play an important role for every M_S in the allowed regions of Fig. 3, (ii) in contrast to standard and shifted FHI, $|dn_s/d \ln k|$ is considerably enhanced with $-0.005 \gtrsim dn_s/d \ln k \gtrsim -0.01$ holding in a sizable portion of the parameter space for $v_G \sim M_{\text{GUT}}$, (iii) the constraint of Eq. (21) does not restrict the parameters unlike the cases of standard and shifted FHI (on the dashed lines we have $0.02 \lesssim M_S/(5 \times 10^{17} \text{ GeV}) \lesssim 1.05$, $12.6 \lesssim N_{\text{HI}^*} \lesssim 21.3$, whereas $N_{\text{HI}^*}^{\text{min}} \sim 10$ –11), and (iv) as in the case of shifted FHI, we can find an acceptable solution fixing $n_s = 0.958$ and $v_G = M_{\text{GUT}}$ (some key inputs and outputs of this solution are arranged in Table II).

7. CONCLUSIONS

We investigated a cosmological scenario tied to two bouts of inflation. The first one is a GUT scale FHI which reproduces the current data on $P_{\mathcal{R}}$ and n_s within the power-law Λ CDM cosmological model and generates

a limited number of e-foldings N_{HI^*} . The second one is an intermediate scale MI which produces the residual number of e-foldings. We assume that the field which is responsible for MI is a string axion which remains naturally almost massless during FHI. We have taken into account extra restrictions on the parameters originating from (i) the resolution of the horizon and flatness problems of the standard big bang cosmology, (ii) the requirements that FHI lasts long enough to generate the observed primordial fluctuations on all the cosmological scales and that these scales are not reprocessed by the subsequent MI, (iii) the limit on the running of n_s , (iv) the naturalness of MI, (v) the homogeneity of the present universe, and (vi) the complete randomization of the string axion during FHI. Fixing n_s to its central value, we concluded that (i) relatively large κ 's and v_G 's are required within the standard FHI with $10 \lesssim N_{\text{HI}^*} \lesssim 21.7$ and (ii) identifica-

tion of the GUT breaking VEV with the SUSY GUT scale is possible within shifted [smooth] FHI with $N_{\text{HI}^*} \simeq 21$ [$N_{\text{HI}^*} \simeq 18$]. In all these cases, MI of the slow-roll type with $m_s/H_s \sim 0.6 - 0.8$ and a very mild tuning (of order 0.01) of the initial value of the string axion produces the necessary additional number of e-foldings. Therefore, MI complements successfully FHI.

Acknowledgments

We would like to thank K. Dimopoulos and R. Trotta for useful discussions. This work has been supported by the European Union under the contracts MRTN-CT-2004-503369 and HPRN-CT-2006-035863 as well as by the PPARC research grant PP/C504286/1.

-
- [1] D.N. Spergel *et al.*, *astro-ph/0603449*.
[2] G. Lazarides, *hep-ph/0011130*; R. Jeannerot, S. Khalil, and G. Lazarides, *hep-ph/0106035*.
[3] E.J. Copeland, A.R. Liddle, D.H. Lyth, E.D. Stewart, and D. Wands, *Phys. Rev. D* **49**, 6410 (1994) [*astro-ph/9401011*].
[4] G.R. Dvali, Q. Shafi, and R.K. Schaefer, *Phys. Rev. Lett.* **73**, 1886 (1994) [*hep-ph/9406319*]; G. Lazarides, R.K. Schaefer, and Q. Shafi, *Phys. Rev. D* **56**, 1324 (1997) [*hep-ph/9608256*].
[5] V.N. Şenoğuz and Q. Shafi, *Phys. Lett. B* **567**, 79 (2003) [*hep-ph/0305089*]; *ibid.* **582**, 6 (2003) [*hep-ph/0309134*].
[6] L. Boubekeur and D. Lyth, *J. Cosmol. Astropart. Phys.* **07**, 010 (2005) [*hep-ph/0502047*].
[7] M. Bastero-Gil, S.F. King, and Q. Shafi, *hep-ph/0604198*; M. ur Rehman, V.N. Şenoğuz, and Q. Shafi, *Phys. Rev. D* **75**, 043522 (2007) [*hep-ph/0612023*].
[8] B. Garbrecht, C. Pallis, and A. Pilaftsis, *J. High Energy Phys.* **12**, 038 (2006) [*hep-ph/0605264*].
[9] R.A. Battye, B. Garbrecht, and A. Moss, *J. Cosmol. Astropart. Phys.* **09**, 007 (2006) [*astro-ph/0607339*].
[10] G. Lazarides, R. Ruiz de Austri, and R. Trotta, *Phys. Rev. D* **70**, 123527 (2005) [*hep-ph/0409335*].
[11] R. Jeannerot and M. Postma, *J. High Energy Phys.* **05**, 071 (2005) [*hep-ph/0503146*].
[12] J. Rocher and M. Sakellariadou, *J. Cosmol. Astropart. Phys.* **03**, 004 (2005) [*hep-ph/0406120*].
[13] P. Binétruy and M.K. Gaillard, *Phys. Rev. D* **34**, 3069 (1986); F.C. Adams, J.R. Bond, K. Freese, J.A. Frieman, and A.V. Olinto, *ibid.* **47**, 426 (1993) [*hep-ph/9207245*]; T. Banks, M. Berkooz, S.H. Shenker, G.W. Moore, and P.J. Steinhardt, *ibid.* **52**, 3548 (1995) [*hep-th/9503114*]; R. Brustein, S.P. De Alwis, and E.G. Novak, *ibid.* **68**, 023517 (2003) [*hep-th/0205042*].
[14] M.Yu. Khlopov and A.D. Linde, *Phys. Lett. B* **138**, 265 (1984); J. Ellis, J.E. Kim, and D.V. Nanopoulos, *ibid.* **145**, 181 (1984).
[15] T.W.B. Kibble, *J. Phys. A* **9**, 387 (1976).
[16] K. Benakli and S. Davidson, *Phys. Rev. D* **60**, 025004 (1999) [*hep-ph/9810280*].
[17] M. Kawasaki, M. Yamaguchi, and J. Yokoyama, *Phys. Rev. D* **68**, 023508 (2003) [*hep-ph/0304161*]; M. Yamaguchi and J. Yokoyama, *ibid.* **68**, 123520 (2003) [*hep-ph/0307373*]; *ibid.* **70**, 023513 (2004) [*hep-ph/0402282*]; M. Kawasaki, T. Takayama, M. Yamaguchi, and J. Yokoyama, *ibid.* **74**, 043525 (2006) [*hep-ph/0605271*].
[18] A.D. Linde, *Phys. Lett. B* **108**, 389 (1982); A. Albrecht and P.J. Steinhardt, *Phys. Rev. Lett.* **48**, 1220 (1982).
[19] R. Jeannerot, S. Khalil, G. Lazarides, and Q. Shafi, *J. High Energy Phys.* **10**, 012 (2000) [*hep-ph/0002151*].
[20] G. Lazarides and C. Panagiotakopoulos, *Phys. Rev. D* **52**, 559 (1995) [*hep-ph/9506325*]; G. Lazarides, C. Panagiotakopoulos, and N.D. Vlachos, *ibid.* **54**, 1369 (1996) [*hep-ph/9606297*]; R. Jeannerot, S. Khalil, and G. Lazarides, *Phys. Lett. B* **506**, 344 (2001) [*hep-ph/0103229*].
[21] G. Ballesteros, J.A. Casas, and J.R. Espinosa, *J. Cosmol. Astropart. Phys.* **03**, 001 (2000) [*hep-ph/0601134*].
[22] V.N. Şenoğuz and Q. Shafi, *Phys. Rev. D* **71**, 043514 (2005) [*hep-ph/0412102*]; *hep-ph/0512170*.
[23] G. Lazarides, *Lect. Notes Phys.* **592**, 351 (2002) [*hep-ph/0111328*]; *J. Phys. Conf. Ser.* **53**, 528 (2006) [*hep-ph/0607032*].
[24] A. Linde, *J. High Energy Phys.* **11**, 052 (2001) [*hep-th/0110195*].
[25] C.P. Burgess, R. Easther, A. Mazumdar, D.F. Mota, and T. Multamaki, *J. High Energy Phys.* **05**, 067 (2005) [*hep-th/0501125*].
[26] U. Seljak, A. Slosar, and P. McDonald, *J. Cosmol. Astropart. Phys.* **10**, 014 (2006) [*astro-ph/0604335*].
[27] A.A. Starobinsky and J. Yokoyama, *Phys. Rev. D* **50**, 6357 (1994) [*astro-ph/9407016*]; E.J. Chun, K. Dimopoulos, and D. Lyth, *ibid.* **70**, 103510 (2004) [*hep-ph/0402059*].
[28] M. Dine, L. Randall, and S. Thomas, *Phys. Rev. Lett.* **75**, 398 (1995) [*hep-ph/9503303*]; M.K. Gaillard, H. Murayama, and K.A. Olive, *Phys. Lett. B* **355**, 71 (1995) [*hep-ph/9504307*].
[29] K.I. Izawa, M. Kawasaki, and T. Yanagida, *Phys. Lett. B* **411**, 249 (1997) [*hep-ph/9707201*]; M. Kawasaki, N. Sugiyama, and T. Yanagida, *Phys. Rev. D* **57**, 6050 (1998) [*hep-ph/9710259*]; M. Kawasaki and T. Yanagida, *ibid.* **59**, 043512 (1999) [*hep-ph/9807544*].